Sensors and Materials, Vol. 36, No. 4 (2024) 1359–1375
MYU Tokyo

S & M 3604

Optimal Prediction of Effectiveness of Mangrove Forest Against Coastal Erosion: Case Study of Coastal Area along the Gulf of Thailand

Puangpet Rattanarama,[1*] Chalida U-tapao,[1]
Yoshimichi Yamamoto,[2] and Arj-ong Nopmuang[2]

[1]Department of Civil Engineering, School of Engineering, King Mongkut's Institute of Technology Ladkrabang,
1 Chalongkrung, Ladkrabang, Bangkok 10520, Thailand
[2]School of Architecture and Urban Planning, Department of Civil Engineering, Tokai University,
4-1-1 Kitakaname, Hiratsuka-shi, Kanagawa 259-1292 Japan

(Received September 11, 2023; accepted February 1, 2024)

Keywords: mangrove, *Rhizophora mucronata*, coastal erosion, sociological impact, Gulf of Thailand

Coastal erosion in Thailand is severe due to the deforestation of mangrove forests, which naturally dissipate waves, making it necessary to establish how to reproduce mangrove forests of a suitable size. First, a survey of mangrove forests was performed in 2012–2013 along the coast of the Gulf of Thailand, where mangrove vegetation has been affected by human activities. The survey showed that tentacle-root mangroves (*Rhizophora mucronata*) accounted for the largest proportion of the mangrove trees in the area. The distribution characteristics of the root number per mangrove tree and the diameters of root systems and main trunks were also clarified. The parametric results were used to make replicas of mangrove vegetation. Hydraulic experiments were carried out in a wave tank in 2014, and a calculation diagram for obtaining the wave transmission ratio was constructed, which was improved over 2015–2018. Moreover, experimental data of eight existing papers were used to increase the value and reliability of this diagram. As a result, a wave transmission ratio can be obtained as a function of the density of mangrove vegetation and the ratio of the incident wavelength to the offing direction width of a mangrove forest. Next, the wave transmission ratio of existing detached breakwaters made of geotextile sandbags was evaluated by simulation using the numerical model [V. T. Ca: VNU J. Sci., Earth Sci. **23** (2007) 160], then the required width of a mangrove forest for it to have the same effect as an existing detached breakwater was estimated. The wave transmission ratio of this breakwater was 0.33, and the offing direction width of the tentacle-root mangrove forest was 250 m with a tree density of 0.8 (the number of trees/m^2). By performing verification simulations using experimental data, the high reproduction accuracy of the topographical changes obtained by the numerical model of Ca *et al.* was confirmed.

*Corresponding author: e-mail: ramaratt@yahoo.com
https://doi.org/10.18494/SAM4653

ISSN 0914-4935

1. Introduction

Many types of solid breakwaters are used to prevent coastal erosion in Thailand. Most breakwaters require a large budget to construct, and concrete breakwaters are not suitable for the clay coasts of Thailand. These solid breakwaters interfere with the lives of people living along the coast and are a common source of complaint. The Department of Marine and Coastal Resources in Thailand is taking a serious look at the study of mangrove forests. Mangrove forests are a natural dam that is suitable, reasonable, and sustainable for Thailand and can be planted easily with low budget. For example, fishermen can pass through mangrove forests in small boats, and some of the roots of mangroves can be removed to provide a passage to the sea; these roots can regrow to support the mangrove trunk. The mature seeds of mangroves fall into the mud, enabling the growth of further trees. The roots of mangrove trees act as a soft buffer for coasts. Moreover, they are a suitable habitat for a wide variety of fish, shrimps, crabs, and other marine animals, providing an important food source for local people. This study confirms the importance of mangrove forests for people and for preventing coastal erosion.

In Thailand, the soil surface elevation in and near mangrove forests has increased in response to local rises in sea level. Annual elevation rates range from 1–10 mm, depending on the coastal area, namely, on sedimentation rates and subsurface mangrove roots. McIvor *et al.* used the surface elevation table and marker horizon method to find that, in many areas, mangrove soil surfaces elevation have increased relative to ocean levels.(1)

Mazda *et al.* reported that wave heights decrease by up to 20% for every 100 m of coastal vegetation.(2) Das *et al.* and Riley *et al.* investigated the constrained comprehension of waveforms in mangrove forests through hypothetical and field examinations, and proposed a numerical model to characterize the dissipation of irregular, wind-driven surface waves in mangrove areas.(3,4)

Specifically, in this research, we conducted a field survey of mangrove forests along a coastal area of the Gulf of Thailand. By the field survey, we first determined the most abundant mangrove species in the area and characterized the number of roots per mangrove tree and the diameters of the root system and main trunk. *Rhizophora mucronata* (a specific mangrove species) was chosen because it has a special root system similar to the tentacles of an octopus that can support the mangrove trunk under various wave conditions. The above-water roots are the upper part of the roots of *Rhizophora mucronata*. They spread radially around the trunk and support the trunk in the same way as flying buttresses. Moreover, they are sufficiently porous to absorb and release water, than blocking it, in contrast to a general solid breakwater (concrete breakwater, geotextile sandbag).

The findings were used to make mangrove replicas, and hydraulic experiments were performed in a wave tank to construct a calculation diagram for obtaining the wave transmission ratio as a function of the mangrove vegetation density and the ratio of the incident wavelength to the offing direction width of a mangrove forest. Further numerical simulations were then carried out under the conditions of no countermeasures, the existing detached breakwater made of geotextile sandbags, and a mangrove forest. We confirmed the effectiveness of the existing detached breakwater for coastal erosion prevention and that a mangrove forest with an offing direction width of 250 m and a density of 0.8 trees/m^2 has the same effect as the existing detached breakwater.

Capacitance wave meters manufactured by Kenek Co. Ltd. were used to measure the wave height, and topographic changes were captured with a Sony high-resolution video camera to obtain changes in the ground height.

For coastal engineers to accurately reproduce the topographic changes for each wave, the tidal changes at the target time are also important. However, the numerical simulation model of beach changes in the 2D plane requires almost the same calculation time as real time because the calculation by this model uses irregular wave data, thus requiring an enormous amount of computation. Therefore, if wave data and tidal change data are input for the numerical calculation over a year, the actual calculation time will be at least one year. Such a method is not practical for evaluating the effectiveness of erosion prevention measures. Therefore, we examine the erosion prevention effect for a half-day storm surge, during which there are large waves, which occurs once a year. In this case, the tide level changes from high tide to low tide; thus, the mean tide level is used.

2. Field Survey of Mangrove Forests

Figure 1 shows a map of the study area along the Gulf of Thailand, which is abundant in mangroves. The study area covers 10 provinces: Chanthaburi (Kung Grabain Bay), Rayong (Prasae Estuary), Chonburi (Laem Chabang), Samut Prakan (Klong Dan), Samut Sakhon (Khok Kham), Petchaburi (Leamluang; Laem Pak Bia), Prachuab Khirikhan (Ban Khao Daeng), Chumphon (Tha Sala), Surat Thani (Leam Pho; Tha Chang; Paknam Ka Dae), and Nakhon Si Thammarat (Ban Bang Pu). These areas were surveyed in 2013. The tide levels were checked from reports of the Department of Marine and Coastal Resources, but we were only interested in the actual distribution of mangroves in our field survey and did not measure the effectiveness of erosion prevention at each site; thus, detailed tide level data was unnecessary.

In Thailand, mangrove forest destruction is attributable to both natural and anthropogenic causes, as follows.

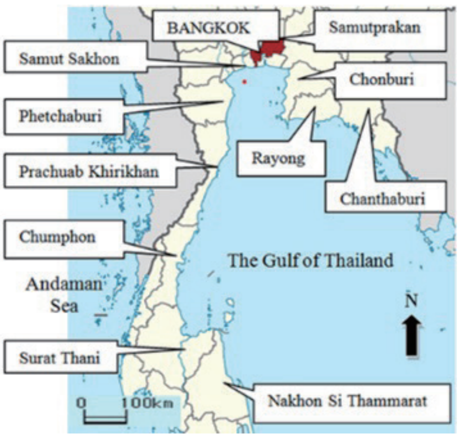

Fig. 1. (Color online) Map of study areas on the eastern, western, and upper parts along the coastline of the Gulf of Thailand.

1) Storm surges are mainly responsible for the destruction of mangroves along the Gulf of Thailand. A storm surge brings about floods, causes damage to plantation areas, and affects the livelihoods of local residents. The intensity of the damage is directly correlated with the extent of mangrove destruction. Strong winds can also uproot mangrove trees along the coastline.
2) Human activity also contributes to the deterioration of mangrove forests on the coastal area along the Gulf of Thailand. The construction of luxury hotels and beach resorts to cater to tourists accelerates their destruction, as the seashore is developed into tourist accommodation and seaside restaurants. Shrimp farming also contributes to the large-scale destruction of mangroves and the local marine ecosystem. The situation is worsening as the global demand for shrimps increases.

Table 1 tabulates the areas of mangroves in the regions of interest along the Gulf of Thailand between 1971 and 2009. The alarming decline in mangrove vegetation is largely attributable to human activities, particularly the construction of seaside accommodation and infrastructure to cater to tourists and industrial-scale shrimp farms. The situation, however, has gradually improved since 1991, when the public and private sectors launched mangrove reforestation programs, such as the Plant Genetic Conservation Project under the Royal Patronage of Her Royal Highness Princess Maha Chakri Sirindhorn.

Figures 2 and 3 respectively depict tentacle-root mangrove vegetation (*Rhizophora mucronata*) in Surat Thani province and *Rhizophora apiculata* in Chanthaburi province. Figures 4 and 5 respectively depict mangrove vegetation with spike breathing roots (*Avicennia sonneratia*) and mangrove trees with buttress roots (*Xylocarpus granatum Koenig*).

Tentacle-root mangroves (*Rhizophora mucronata*) are considerably more abundant than other types of mangrove along the coastal area of the Gulf of Thailand. In addition, *Rhizophora mucronata* is a fast-growing plant species and requires low maintenance. Thus, we focus mainly on the tentacle-root mangroves. Moreover, the tree density (the number of mangroves per square meter) of natural tentacle-root mangrove forests is about 0.3 and that of artificial forests is 0.5 (large forests) to 1.0 (small forests).

Table 1
Areas of mangrove forest along the coastline of the Gulf of Thailand (source: Department of Marine and Coastal Resources of Thailand).

Province	1971	1975	1979	1986	1989	1991	1996	2000	2004	2009
	km^2	km^2	km^2	km^2	km^2	km^2	km^2	km^2	km^2	km^2
Chanthaburi	154.00	261.00	240.64	145.42	86.96	26.95	38.93	125.73	117.94	120.69
Rayong	17.00	55.00	46.08	24.18	17.58	1.54	6.56	18.82	13.93	18.05
Samut Prakarn	—	6.00	8.80	1.03	—	—	2.97	11.55	14.66	20.04
Chonburi	—	38.00	4.32	14.98	8.93	1.50	0.92	7.34	7.22	8.89
Samut Sakhon	—	185.00	144.16	1.42	—	—	16.96	30.80	21.85	40.41
Petchaburi	22.00	88.00	77.92	5.77	4.89	3.36	20.70	30.67	10.48	29.71
Prachuab Khirikhan	11.00	4.16	3.36	1.45	1.10	0.70	0.43	5.00	4.33	2.75
Chumphon	81.00	74.00	69.28	36.29	22.65	18.18	31.84	72.47	64.86	51.56
Surat Thani	256.00	37.00	58.08	42.84	37.67	22.04	31.82	93.00	52.02	74.52
Nakhon Si Thammarat	612.00	155.00	128.32	88.36	93.21	80.25	84.16	94.20	140.96	117.68

Fig. 2. (Color online) Mangrove vegetation with tentacle roots (*Rhizophora mucronata*) in Tha Chang district, Surat Thani province.

Fig. 3. (Color online) Mangrove vegetation (*Rhizophora apiculata*) in Kung Krabain Bay, Chanthaburi province.

Fig. 4. (Color online) Mangrove vegetation with spike breathing roots (*Avicennia sonneratia*) in Klong Dan region, Samut Prakan province.

Fig. 5. (Color online) Mangrove trees with buttress roots (*Xylocarpus granatum Koenig*) in Kho Kud, Trad province.

3. Statistical Values Based on Field Survey Results

The field survey was carried out in the study area along the coastline of the Gulf of Thailand to quantify tentacle-root mangrove trees in terms of the number of above-water roots per tree and the diameters of the root system and main trunk.

Figure 6 illustrates the frequency distribution of the number of above-water roots (1 m or longer in length) per tree for tentacle-root mangroves. Mangrove trees with 10–20 roots accounted for the largest proportion, and the average diameter of individual roots was 2 cm.

Figure 7 depicts the frequency distribution of the diameter of the entire root system for tentacle-root mangroves. The most prevalent diameter was around 200 cm.

Figure 8 shows the frequency distribution of the diameter of the main trunk for tentacle-root mangroves. The most common trunk diameter is 8 cm, indicating that the age of mangroves along the coastal area of Thailand is between 4 and 10 years.

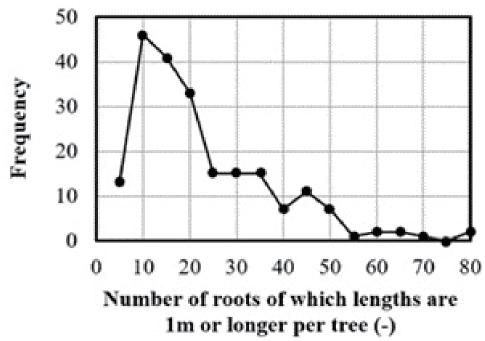

Fig. 6. Frequency distribution of number of above-water roots (1 m or longer) per tree for tentacle-root mangroves. (Above-water roots are the upper part of mangrove roots, which are not under water or clay, Fig. 2.)

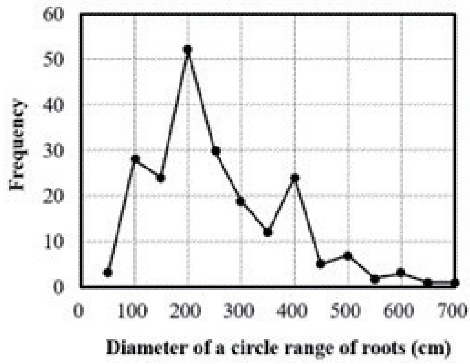

Fig. 7. Frequency distribution of the diameter of the entire root system for tentacle-root mangroves.

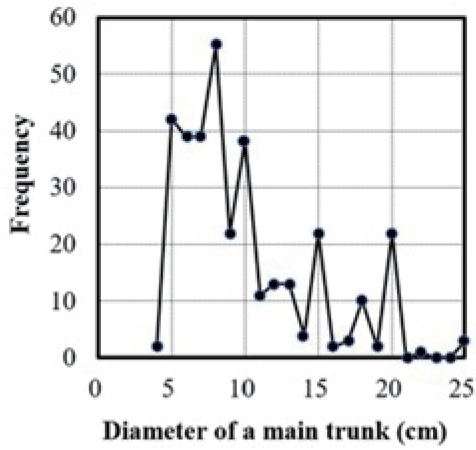

Fig. 8. Frequency distribution of the diameter of the main trunk for tentacle-root mangroves.

The highest scores are shown in Figs. 6–8 when we surveyed the real sites along the Gulf of Thailand (Fig. 1). The replica of the roots of the mangrove tree (*Rhizophora mucronata*) can be made for the simulation in wave tank.

4. Calculation Diagram for Obtaining Wave Transmission Ratios

Ca *et al.* developed a 2D numerical simulation model that can predict topographical changes along a coast due to incident irregular waves and can evaluate the effect of wave dissipation by coastal structures on topographical changes.[5,6] Yamamoto *et al.* confirmed the high reproduction accuracy of the numerical model of Ca *et al.* for sandy coasts.[7] However, when evaluating the wave dissipation effect by coastal structures, suitable ratios of wave dissipation by coastal structures must be set in the simulation. Therefore, Charusrojthanadech *et al.* proposed a method of evaluating the wave dissipation ratios of detached breakwaters made of bamboo piles and those made of geotextile sandbags in Thailand.(8) Moreover, Rattanarama *et al.* constructed a calculation diagram for obtaining the transmission ratio of the significant wave height from the offing direction width of a mangrove forest.(9)

However, if the ratio of the incident wavelength to the offing direction width of the mangrove forest changes, even if the incident wave height is the same, the transmission ratio must also change. For example, Alongi pointed out that a change in the period of the incident wave affects the relationship between the transmission ratio and the width of the mangrove forest, and indicated that the transmission ratio becomes 0.5 when the width of the dense mangrove forest is around 50 m and the incident wave period is 2–3 s or when the width of the loose mangrove forest is around 400 m and the incident wave period is 8 s.(10)

Therefore, we reconstructed the calculation diagram for obtaining the transmission ratio of the significant wave height from the ratio of the incident wavelength to the offing direction width of the mangrove forest by combining data obtained from our hydraulic experiments for a small offing direction width of the mangrove forest and experimental data from existing papers in which the offing direction width was large.

In our hydraulic experiments, 1:10 scale replicas of tentacle-root mangrove vegetation were made on the basis of the survey data for the number of roots per tree and the root system and trunk diameters, as shown in Fig. 9. The wave tank shown in Fig. 13 (22.0 m length, 0.8 m height, 0.5 m width) was used, and mangrove trees and four wave gauges (for measuring incident and reflection wave heights) were installed, as shown in Fig. 14. The mangrove replicas were fixed by placing them in a soil bed of 10 cm thickness (median diameter of 0.2 mm and uniformity coefficient of 20) and the water depth was around 30 cm (corresponding to 3.0 m in the field).

The incident significant wave height was 18 cm (1.8 m in the field) and the wave period was 1.25 s (4.0 s in the field). Hydraulic experiments were performed with tree densities of 0.3, 0.5, and 1.0 (per m^2) and nondimensional widths (ratio of the offing direction width of mangrove forest to incident wavelength) of 0.5, 1.0, and 2.0. The experimental results are given in the upper half of Table 2.

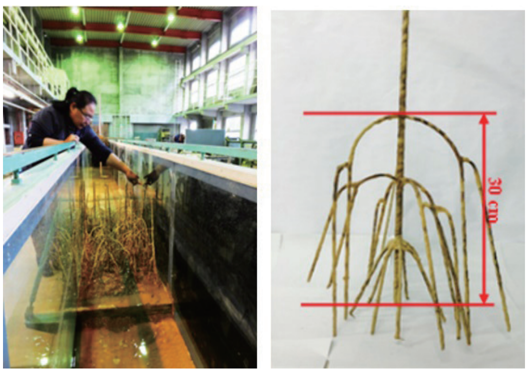

Fig. 9. (Color online) Replica of a mangrove tree and installation of the replicas in a wave tank (1:10 scale).

Fig. 10. (Color online) Installation of the replicas in a wave tank (1:10 scale).

Fig. 11. (Color online) Replicas in water at the normal level.

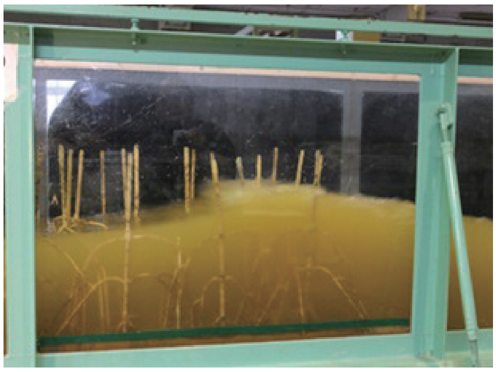

Fig. 12. (Color online) Simulation waves approaching the replicas in the mangrove forest in the wave tank.

Fig. 13. (Color online) Complete view of the wave tank, which can generate irregular waves with significant wave heights of 0–25 cm.

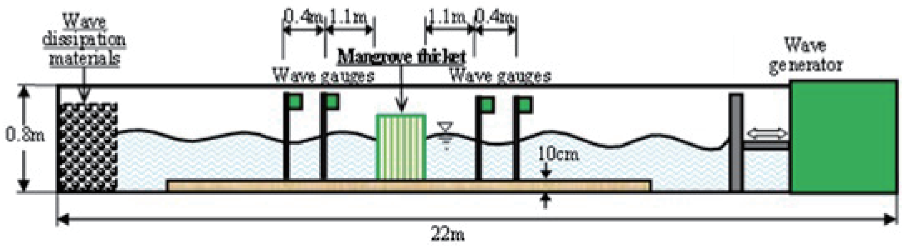

Fig. 14. (Color online) Illustration of the wave tank and setup of mangrove trees and four wave gauges.

We plotted data from the studies of Brinkman, Fatimah *et al.*, Narayan, Tuyen and Hung, Bao, Suzuki, McIvor *et al.*, and Kristiyanto *et al.* on a graph (x-axis: nondimensional width, y-axis: wave transmission ratio), then drew three curves plotting the wave transmission ratios and nondimensional widths corresponding to tree densities of 0.3, 0.5, and 1.0.[11–18] Next, we obtained the wave transmission ratios corresponding to the nondimensional widths of 9.1, 18.2,

Table 2
Wave transmission ratio as a function of tree density and nondimensional width of mangrove forest.

	Nondimensional width of mangrove forest (mangrove forest offing direction width/incident wavelength)	Wave transmission ratio (significant transmission wave height/significant incident wave height)		
		Tree density = 0.3	Tree density = 0.5	Tree density = 1.0
Data of our hydraulic experiments	0	1.00	1.00	1.00
	0.5	0.94	0.92	0.91
	1.0	0.92	0.90	0.88
	2.0	0.89	0.84	0.79
Experimental data of previous papers	9.1	0.80	0.65	0.39
	18.2	0.70	0.49	0.20
	27.3	0.62	0.39	0.12
	36.4	0.55	0.31	0.07
	45.5	0.50	0.25	0.03
	54.6	0.45	0.21	0.00
	63.7	0.43	0.20	0.00

27.3, 36.4, 45.5, 54.6, and 63.7 from the three curves. The obtained data are given in the lower half of Table 2.

Using the data in Table 2, we constructed the calculation diagram for obtaining the wave transmission ratio from the density of tentacle-root mangrove trees and the nondimensional width of the mangrove forest, as shown in Fig. 15. Here, the densities of 0.3 and 1.0 are equivalent to the densities of natural and artificial forests, respectively.

5. Confirmation of Reproducibility of Model of Ca *et al.*

In this section, we confirm the reproducibility of the numerical simulation model of Ca *et al.* for a soil coast that includes silt.[5,6]

First, we performed some hydraulic experiments on topographical changes of the soil coast without and with a mangrove thicket due to irregular waves using the wave tank and the model shown in Fig. 16.

A soil beach with a slope of 1:20 was made using soil with a median particle diameter of 0.2 mm and a uniformity coefficient of 20, and a mangrove thicket with a width of 0.8 m (8.0 m in the field) was installed in the offing direction from a position 1.4 m from the shoreline. The tree density (number of trees per m^2) of the mangrove thicket was 0.01 (1.0 in the field, corresponding to an artificial forest) and the water depth was 30 cm.

Then, irregular waves of 18 cm significant wave height and 1.2 s wave period were generated, and the volume of beach erosion between the mangrove thicket and the shoreline was measured after 60, 120, and 180 min. For the case with a mangrove thicket, since the volume of coastal erosion was small, the experiment was performed three times.

The beach erosion in the case of no mangrove thicket is shown in Fig. 17, and the beach erosion in the case of a mangrove thicket for the three repeated experiments is shown in Figs. 18–20. The measured volume of beach erosion for all cases is given in Table 3.

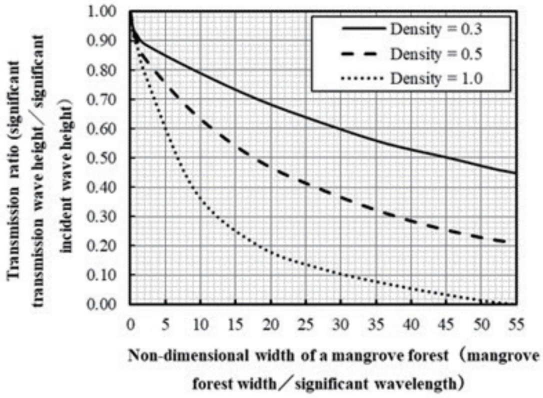

Fig. 15. Calculation diagram for obtaining wave transmission ratio for mangrove trees.

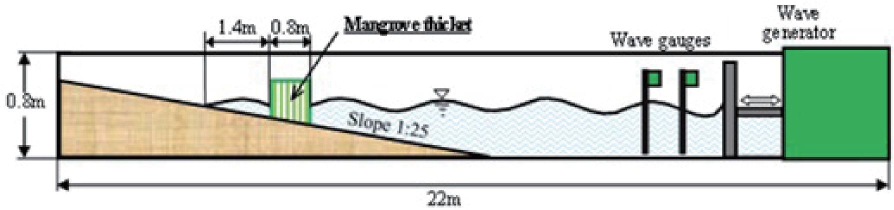

Fig. 16. (Color online) Illustration of the wave tank and the model for experiments on topographical changes of a soil beach.

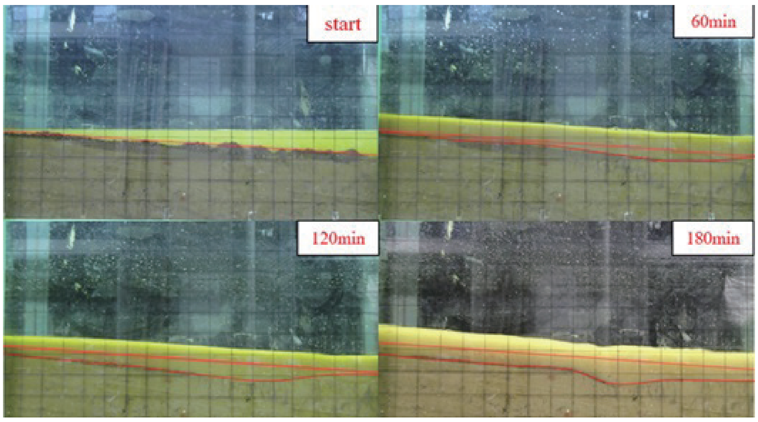

Fig. 17. (Color online) Experimental results for case without the mangrove thicket.

Next, we attempted to reproduce the beach erosion in the hydraulic experiments by using the numerical model of Ca *et al.*[5,6] Since this model is solved by the finite difference method, and the energy spectrum is used to handle irregular waves, for the reproduction simulations, we changed the mesh interval to 8 cm and the spreading parameter (S_{max}) to 25. The wave transmission ratio was found to be 0.88 by applying the ratio of the mangrove forest width to the

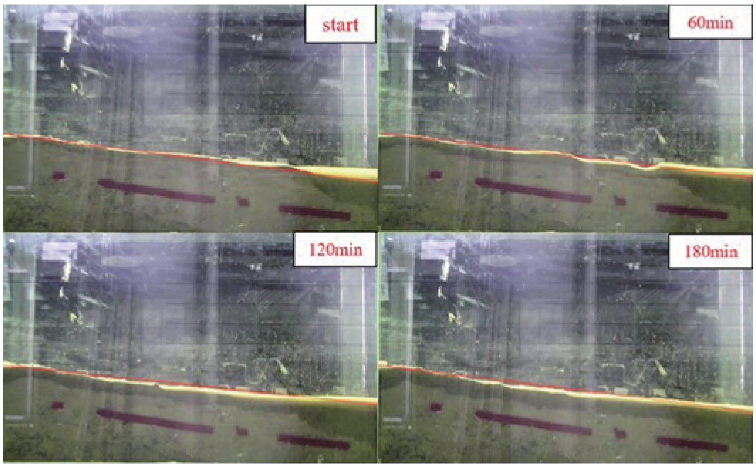

Fig. 18. (Color online) Experimental results with the mangrove thicket (first time).

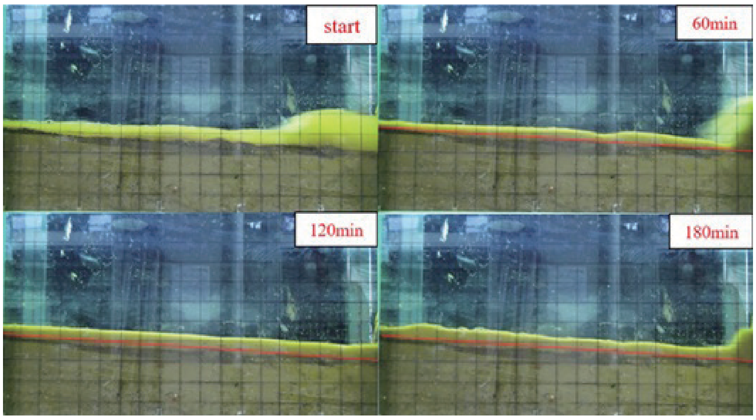

Fig. 19. (Color online) Experimental results with the mangrove thicket (second time).

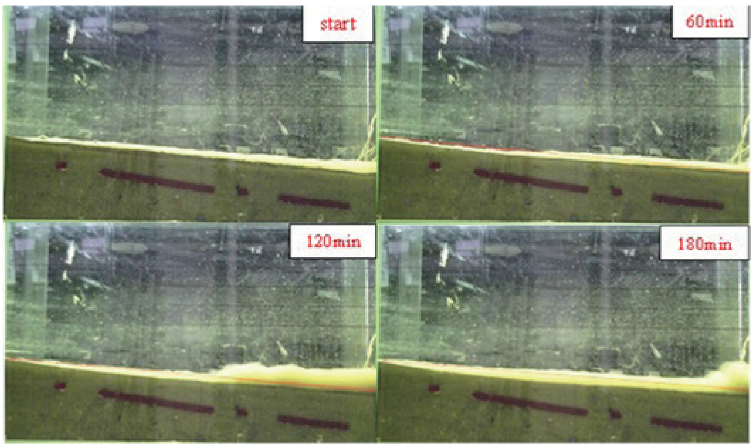

Fig. 20. (Color online) Experimental results with the mangrove thicket (third time).

Table 3
Measured and calculated volumes of beach erosion between mangrove thicket and shoreline.

Elapse time (min)	Beach erosion volume per unit length (cm^3/cm)						
	Without mangrove thicket		With mangrove thicket				
	Measured value	Calculated value	Measured value				Calculated value
			1st time	2nd time	3rd time	Average	
60	43.0	70	5.7	6.8	7.1	6.5	11
120	91.0	120	7.8	9.0	8.9	8.6	22
180	191.5	200	8.1	11.6	10.9	10.2	35

incident wavelength (= 1.0) and the tree density (= 1.0/1 m) to Fig. 15. The calculation results for the wave height are shown in Fig. 21 (left: no mangrove thicket; right: mangrove thicket) and the calculation results for the topographical changes are shown in Fig. 22 (left: no mangrove thicket; right: mangrove thicket).

The calculated volume of beach erosion between the mangrove thicket and the shoreline is given in Table 3, and the relationship between the calculated volume and the measured volume is shown in Fig. 23. Although the numerical model of Ca *et al.* overestimates the volume of beach erosion, because the correlation coefficient is 0.99, we can conclude that the reproducibility of the numerical model of Ca *et al.* for the soil coast is sufficiently high.[5,6]

6. Suitable Width of a Mangrove Forest

In this section, we clarify the suitable width of a mangrove forest by using the numerical model of Ca *et al.*[5,6]

Detached breakwaters made of geotextile sandbags, as shown in Fig. 24, were constructed to prevent coastal erosion on the Klong Dan coast in Bangkok Bay, which reduced the mean water depth of the sea on the land side of the detached breakwaters to about 1 m. Therefore, we consider that a mangrove forest will have the same erosion prevention capability as the detached breakwaters made of geotextile sandbags.

First, we reproduced the erosion prevention capability of one of these detached breakwaters (2.5 m height × 5.0 m width × 50 m length) using the numerical model of Ca *et al.*[5,6] For the beach profile in this reproduction, the bottom slope was set to 1:200 (the mean slope on the Klong Dan coast) and the diameter of bottom materials was set to 0.1 mm (the median grain size on this coast). The mesh interval of the topographical data was 1.25 m, the incident wave height was 1.25 m (the mean significant wave height during a storm surge according to observation data for 2005, 2006, and 2011), the incident wave period was 3.7 s (the value corresponding to the incident wave height), the spreading parameter (S_{max}) was 25, and the calculation time was 3 days, corresponding to a very long storm.

The results of the topographical calculations are shown in Fig. 25 for two cases: with and without a detached breakwater. Although we assume that this detached breakwater is impermeable, at the time of high tide, since the water surface was 0.5 m higher than the crown height of the detached breakwater, the incident waves can pass over the breakwater. Therefore, numerical simulations were performed for two cases: mean tidal level (water depth in front of

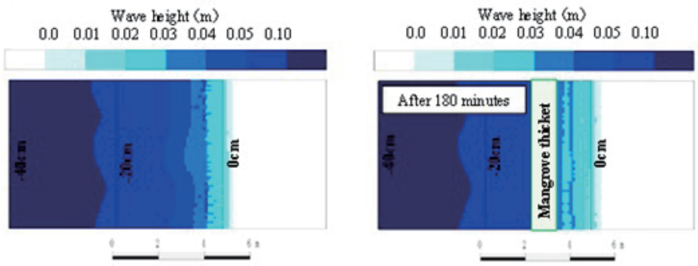

(a) (b)

Fig. 21. (Color online) Calculation results for the wave height for cases of (a) no mangrove thicket and (b) mangrove thicket (right). The left of each figure is the offing side.

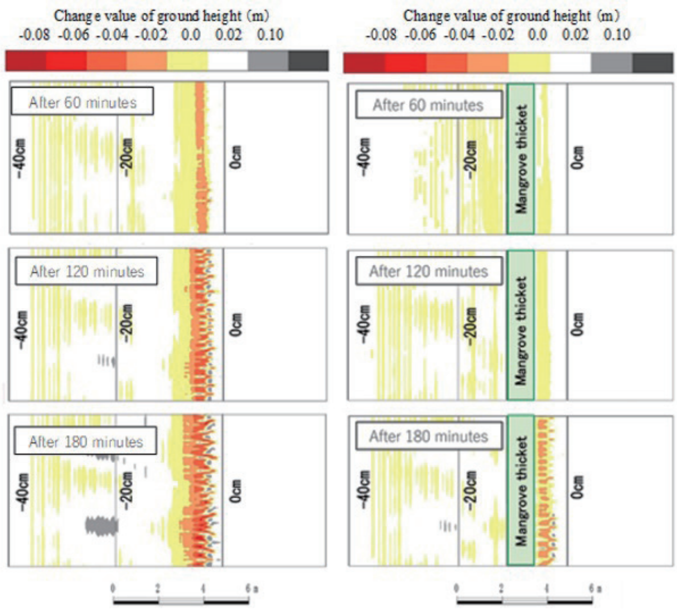

(a) (b)

Fig. 22. (Color online) Calculation results for the topographical change for the cases of (a) no mangrove thicket and (b) mangrove thicket. The left of each figure is the offing side.

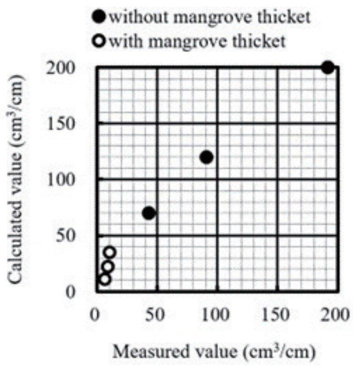

Fig. 23. Relationship between the calculated volume and the measured volume of the beach erosion. The correlation coefficient is 0.99.

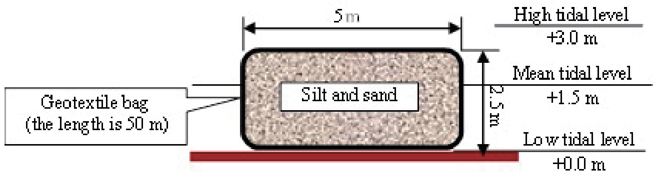

Fig. 24. (Color online) Cross-section view of detached breakwater made of geotextile sandbag.

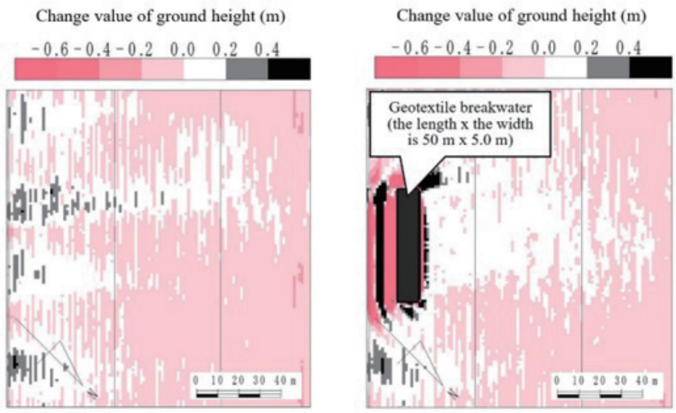

Fig. 25. (Color online) Changes in topography for cases of no geotextile sandbag breakwater and geotextile sandbag breakwater. The left of each figure is the offing side.

detached breakwater of 1.5 m) and high tidal level (water depth in front of detached breakwater of 3.0 m). Then, the weighted average of these simulation results was obtained, as shown in the right of Fig. 25. Here, the weights for the mean tidal level and high tidal level are 5/6 and 1/6, respectively, because the detached breakwater is submerged for one-sixth of the day.

According to Fig. 26, in the area shielded by the detached breakwater, because the erosion of around 10 cm changed to deposition of around 10 cm, it is presumed that the water depth will decrease to about 1 m in some years. Therefore, the reproducibility of the numerical model of Ca *et al.* was shown to be high.[5,6]

Next, we searched for the offing direction width of a mangrove forest with the same erosion prevention capability as the detached breakwater made of geotextile sandbags by repeating the numerical simulation with different offing direction widths. Here, the forest length of 50 m was fixed for comparison with the detached breakwater, and the density of the artificial forest was set to 0.7, because a density of 1.0 is high. In the case of an offing direction width of 250 m, we obtained the same erosion prevention capability as the detached breakwater. In this case, since the nondimensional width was around 23 (width/mean wavelength = 250 m/11 m), the wave transmission ratio was 0.33.

Although the detached breakwater is effective for preventing coastal erosion, the deployment of geotextile sandbags is expensive because of their short lifetime. In contrast, the reproduction of mangrove forests is cost-effective and ecologically sustainable. Moreover, local residents are

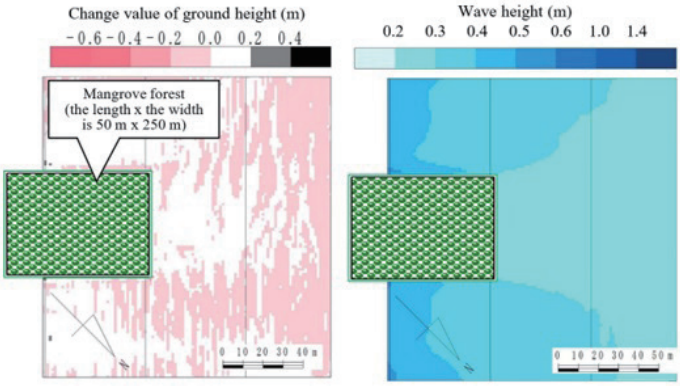

Fig. 26. (Color online) Changes in topography and wave height for case of mangrove forest. The left of each figure is the offing side.

receptive to this environmentally friendly strategy. In addition to preventing coastal erosion, several mangrove forests are also used as tourist attractions.

7. Conclusions

The main conclusions of this study are as follows:

1) We performed a field survey to clarify the characteristics of mangrove forests along the coastal area of the Gulf of Thailand. The survey clarified that tentacle-root mangroves (*Rhizophora mucronata*) constituted the largest proportion of mangroves and that the tree densities are 0.3 (/m^2) for natural mangrove forests, 0.5 for large artificial mangrove forests, and 1.0 for small artificial mangrove forests. Moreover, most tentacle-root mangroves had 10–20 above-water roots (1 m or longer in length) per tree with an average root diameter of 2 cm, a root system diameter of 200–250 cm, and a trunk diameter of 8 cm.
2) When the effect of measures for erosion prevention is evaluated in hydraulic experiments, large experimental facilities, huge cost, and a very long time are required. Since the execution of large-scale experiments is very difficult, as an alternative, numerical simulations can be performed using a simulation model, for which suitable ratios of wave dissipation for different measures are required. Therefore, we performed hydraulic experiments using 1:10 scale replicas of mangrove vegetation and analyzed eight existing papers, and then we proposed a calculation diagram for estimating the wave transmission ratio from the tree density and the nondimensional width of a mangrove forest.
3) Next, we performed hydraulic experiments to obtain verification data for the topographical changes on a soil (silt and sand) coast due to waves, and thus confirmed that the numerical model of Ca *et al.* can accurately reproduce topographical changes on a soil coast.
4) Finally, we reproduced the topographical changes on a soil coast where geotextile detached breakwaters have been installed by using the numerical model of Ca *et al.* We confirmed that the erosion prevention effect of a geotextile detached breakwater is high. We also found that the offing direction width of a mangrove forest with the same erosion prevention effect as a

geotextile detached breakwater is 250 m for a tree density of 0.7 and that the wave transmission ratio in this case is 0.33.

A geotextile detached breakwater has a lifetime of about 10 years, which is the time required for the growth of a replanted mangrove forest until it has sufficient erosion prevention capability. Therefore, we recommend a hybrid measure in which a tentacle-root mangrove forest is replanted in the sea on the land side of geotextile detached breakwaters immediately after their installation.

Acknowledgments

The authors would like to express their deep gratitude to Tokai University, Japan, and King Mongkut's Institute of Technology Ladkrabang (KMITL), Thailand, for research funding. Sincere appreciation also goes to the Department of Marine and Coastal Resources of Thailand, the Royal Thai Survey Department, and the Hydrographic Department of Marine and Coastal Resources for the research facility.

References

1 A. McIvor, T. Spencer, I. Möller, and M. Spalding: Nat. Coastal Prot. Ser. **3** (2013) 1. https://www.conservationgateway.org/ConservationPractices/Marine/crr/library/Documents/mangrove-surface-elevation-and-sea-level-rise.pdf
2 Y. Mazda, M. Magi, M. Kogo, and P. N. Hong: Mangroves Salt Marshes **1** (1997) 127. https://doi.org/10.1023/A:1009928003700
3 P. Das, U. Basak, and A. B. Das: Mangroves Salt Marshes **1** (1997) 155. https://doi.org/10.1023/A:1009980023264
4 R. W. Riley and C. P. S. Kent: Mangroves and Salt Marshes **3** (1999) 207. https://doi.org/10.1023/A:1009963124225
5 V. T. Ca, Y. Yamamoto, K. Tanimoto, and J. Arimura: Coastal Eng. **28** (2002) 1817. https://doi.org/10.1142/9789812791306_0153
6 V. T. Ca: VNU J. Sci., Earth Sci. **23** (2007) 160. https://repository.vnu.edu.vn/bitstream/11126/4550/3/TC_02579.pdf
7 Y. Yamamoto, M. Ioroi, and R. Higa: J. Jpn. Soc. Civ. Eng. B3 **68** (2012) 882. https://doi.org/10.2208/jscejoe.68.I_882
8 N. Charusrojthanadech, P. Rattanarama, and Y. Yamamoto: Int. Offshore Polar Eng. **23** (2013) 1355. https://www.researchgate.net/profile/Yoshimichi-Yamamoto/publication/289852115_Examination_of_coastal_erosion_prevention_in_the_back_of_the_gulf_of_Thailand/links/6437e1c520f25554da2b9529/Examination-of-coastal-erosion-prevention-in-the-back-of-the-gulf-of-Thailand.pdf
9 P. Rattanarama, N. Charusrojthanadech, and Y. Yamamoto: Int. Offshore Polar Eng. **25** (2015) 1365. https://onepetro.org/ISOPEIOPEC/proceedings-abstract/ISOPE15/All-ISOPE15/ISOPE-I-15-553/14852
10 D. M. Alongi: The Energetics of Mangrove Forests (Springer Science, Media B.V., 2009). https://doi.org/10.1007/978-1-4020-4271-3
11 R. M. Brinkman: Wave Attenuation in Mangrove Forests: an Investigation through Field and Theoretical Studies (James Cook University, Australia, 2006)
12 E. Fatimah, A. K. A. Wahab, and H. Ismail: Copedec **7** (2008) 1. https://www.flow3d.com/wp-content/uploads/2014/08/Numerical-modeling-approach-of-an-artificial-mangrove-root-system-ArMs-submerged-breakwater-as-wetland-habitat-protector.pdf
13 S. Narayan: The Effectiveness of Mangroves in Attenuating Cyclone-induced Waves (Delft University of Technology, Netherlands, 2009)
14 N. B. Tuyen, and H. V. Hung: Asian Pacific Coasts **22** (2009) 336. https://doi.org/10.1142/9789814287951_0182
15 T. Q. Bao: Oceanologia **53** (2011) 807. https://doi.org/10.5697/oc.53-3.807
16 T. Suzuki: Wave Dissipation over Vegetation Fields (Delft University of Technology, Netherlands, 2011).
17 A. McIvor, I. Moller, T. Spencer, and M. Spalding: Nat. Coastal Prot. Ser. **1** (2012) 1. https://www.conservationgateway.org/ConservationPractices/Marine/crr/library/Documents/wind-and-swell-wave-reduction-by-mangroves.pdf

18 A. Kristiyanto, H. D. Armono, and Soemarno: Int. J. Eng. Sci. **2** (2013) 2319. https://www.theijes.com/papers/v2-i7/Part.1/C027109017.pdf
19 P. Rattanarama, N. Charusrojthanadech, and Y. Yamamoto: J. Jpn. Soc. Civ. Eng. B2 **69** (2013) 1. https://onepetro.org/ISOPEIOPEC/proceedings-abstract/ISOPE15/All-ISOPE15/14852
20 M. Glaser, U. Berger, and R. Macedo: Reg. Environ. **3** (2003) 162. https://doi.org/10.1007/s10113-003-0057-4
21 Y. Yamamoto, N. Charusrojtanadech, and U. Sirikaew: Int. Offshore Polar Eng. **22** (2012) 1488. https://onepetro.org/ISOPEIOPEC/proceedings-abstract/ISOPE12/All-ISOPE12/ISOPE-I-12-496/12774

About the Authors

Puangpet Rattanarama is a doctoral degree student at the Department of Civil Engineering, School of Engineering, King Mongkut's Institute of Technology Ladkrabang (KMITL), Bangkok, Thailand. She received her bachelor's degree in interior architecture at KMITL in 1991 and her master's degree in Diplom Ingenieur (Innenarchitektur) at Akademie der Bildenden Künste München, Germany, in 1995. She has been a lecturer at the School of Architecture at KMITL since 1981. She has also worked for the Plant Genetic Conservation Project under the Royal Initiative of Her Royal Highness Princess Maha Chakri Sirinthorn since 2005. (ramaratt@yahoo.com)

Chalida U-tapao is an associate professor at King Mongkut's Institute of Technology Ladkrabang (KMITL). Her bachelor's degree was in construction technology at KMITL and her master's degree was in environmental technology at King Mongkut's University of Technology Thonburi. She was awarded a Ph.D. degree in civil and environmental engineering from the University of Maryland at College Park in 2013. (chalida.ut@kmitl.ac.th)

Yoshimichi Yamamoto received B.S., M.S., and Ph.D. degrees from Saitama University, Japan, in 1979, 1981, and 1994, respectively. From 1981 to 2003, he was a senior engineer and researcher at INA, Japan. From 2003 to 2022, he was a professor at School of Architecture and Urban Planning, Tokai University, Japan. Since 2022, he has been a part-time teacher at Tokai University. His research interests are in coastal, port, and river engineering. (yama1231@krd.biglobe.ne.jp)

Arj-ong Nopmueng graduated from King Mongkut's Institute of Technology Ladkrabang with a bachelor's degree in civil engineering in 2012 and from Tokai University with a master's degree in civil engineering in 2015. He then worked for Hitachi Plant Construction in Tokyo, Japan, as a civil engineer responsible for substation, power plant, and chemical plant projects for four years before returning to Thailand to study for an MBA at Chulalongkorn University. He is currently working as a civil engineer in Sato Kogyo Bangkok and is responsible for schedule planning, budget estimation, and project control. (sakurazaki_blm@hotmail.com)